J Nanostruct 13(1): 296-303, Winter 2023

RESEARCH PAPER

Sol-Gel Preparation of Ag_2CoTiO_4 Nanoparticles as Efficient Photocatalyst for Visible Light Degradation of Acid Red 88

*Mehdi Rahbar [1], Molood Barmala [2], Mohammad Behnood [3]**

[1] *Institute of Nanoscience and Nanotechnology, University of Kashan, 87317-51167 Kashan, Iran*

[2] *Department of Chemical engineering, Dezful branch, Islamic Azad University, Dezful, Iran*

[3] *Department of petroleum engineering, science and research branch, Islamic Azad University, Tehran, Iran*

ARTICLE INFO

Article History:
Received 05 October 2022
Accepted 26 December 2022
Published 01 January 2023

Keywords:
Acid red 88
Photocatalyst
Sol-gel
Delafossite structure
Visible light

ABSTRACT

Ag_2CoTiO_4 nanoparticles were synthesized by facile and straightforward sol-gel method. X-ray diffraction analysis reveals that the prepared nanoparticles have hexagonal phase and are truly consistent with delafossite structure. The prepared Ag_2CoTiO_4 nanoparticles possess noticeable absorption in visible light region with energy band-gap of 2.43 eV. The morphological features were studied using SEM and TEM analysis, which show the nano-sized spherical morphology for the prepared nanoparticles. FT-IR spectrum clearly affirms formation of metal-oxygen bonds for the prepared nanoparticles. The photocatalytic potential of the nanoparticles was studied for visible light degradation of acid red 88 (AR 88). After 120 min illumination, the highest photocatalytic activity was attained (89.02%) using 30 mg of the loaded nanoparticles. The effect of different experimental conditions was investigated on the photocatalytic efficiency, including various amount of photocatalyst and concentration of H_2O_2. Recyclability experiment shows that the prepared nanoparticles have a great stability up to 6 consecutive reaction cycles.

How to cite this article
Rahbar M, Barmala M, Behnood M. Sol-Gel Preparation of Ag_2CoTiO_4 Nanoparticles as Efficient Photocatalyst for Visible Light Degradation of Acid Red 88. J Nanostruct, 2023; 13(1):296-303. DOI: 10.22052/JNS.2023.01.029

INTRODUCTION

Owing to remarkable properties, metal oxide nanoparticles have been considered in many technical field including catalytic processes, energy production, water purification, bio-sensing, etc. [1]. In this regard, delafossite compounds have received tremendous attention which is due to vast variety of related structures, excellent electronic and optical properties [2]. These materials belong to a family of ternary oxides with the general formula of $(AB^{2+}_{0.5}C^{4+}_{0.5}O_2)$ (A is a monovalent metal ions, B is a divalent metal ions and C is a tetravalent metal ions) [3].

Over the past few decades, the pollution of water resources has raised serious concerned in the scientific communities worldwide [4]. Hence, developing efficient, non-toxic and affordable photocatalyst materials has been a top priority for research groups [5].

Titanium dioxide (TiO_2) as a common semiconductor photocatalyst has some obstacles that largely restrict its application in the photocatalytic process [6]. The contributing factors that limit photocatalytic activity of TiO_2 are fast recombination of charge carriers, low quantum efficiency and need to shorter wavelength of light spectrum (in UV region) for activation [7]. To solve these above limitations, more efficient

* *Corresponding Author Email: m.behnood@gmail.com*

photocatalyst materials, especially mixed metal oxides, look very promising.

The delafossite compounds have opened the doors for more effective photooxidation of the organic pollutant. For instance, Karati and his colleagues reported the photocatalytic degradation of methylene blue using a series of delafossite-type compounds of $Na_3M_2SbO_6$, where M are transition metals [8]. Guo et al. prepared delafossite silver ferrite photocatalyst and studied its ability for degradation of tetracycline [9].

In this work, we report, for the first time, the sol-gel preparation of Ag_2CoTiO_4 delafossite nanoparticles. The photocatalytic potential of the prepared nanoparticles was investigated for visible-light degradation of acid red 88. The characterization of the prepared nanoparticles was carried out using XRD, SEM, EDX, FT-IR and DRS analysis.

MATERIALS AND METHODS

Preparation of Ag_2CoTiO_4 nanoparticles

The simple sol-gel method was used to synthesize Ag_2CoTiO_4 nanoparticles. First, 2 mL polyethylene glycol (PEG MW = 600) was dissolved into 20 mL ethanol, then 1 mmol of tetrabotyl orthotitanate (TBOT) was added. After stirring for 10 min, 1 mmol of $Co(NO_3)_2.6H_2O$ and 2 mmol of $AgNO_3$ were added to above mixture and stirring was followed for another 30 min. The dark red solution was kept in an oven for overnight at 50 °C. Finally, the dried gel was heated at 350 °C for 24 hours.

Characterization

The phase and structure of the prepared nanoparticles were studied using X-ray diffraction patterns (XRD) (Philips X'pert Pro MPD, Cu *kα* = 1.54 Å). Field emission scanning electron microscopy (FE-SEM) and energy dispersive X-ray (EDX) spectroscopy were performed on TESCAN Mira3 to study the morphology and composition of nanoparticles. Also, morphology of the prepared nanoparticles was investigated using transmission electron microscope (TEM) (Zeiss, EM 900). The chemical groups of the sample was recorded using Fourier transform infrared spectroscopy (FT-IR) (Shimadzu Varian 4300 spectrometer). The optical properties of nanoparticles were studied using UV-Vis diffuse reflectance spectroscopy (DRS) (Shimadzu UV-670).

RESULTS AND DISCUSSION

Fig. 1 shows the XRD pattern for the prepared ACTO nanoparticles. The diffraction peaks at 2ϑ = 14.31°, 28.70°, 34.41°, 35.58°, 39.29°, 42.36°, 48.61°, 52.41°, 59.51°, and 61.29° are truly corresponded to (003), (006), (101), (012), (104), (015), (107), (018), (0012), and (110) planes. This result confirms that the prepared ACTO nanoparticles were crystallized in hexagonal phase of Ag_2CoTiO_4 (JCPDS no. 049-0736). The average

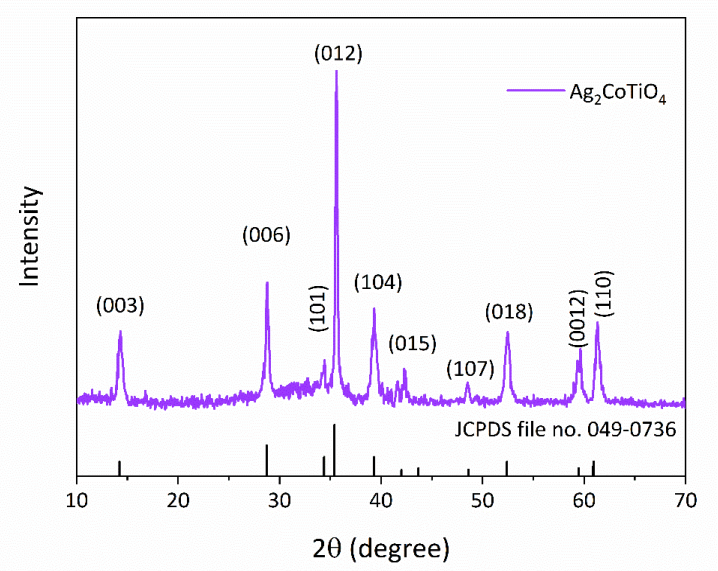

Fig. 1. XRD pattern for the prepared Ag_2CoTiO_4 nanoparticles.

Table. 1. The unit cell parameters and average crystallite size of the prepared Ag_2CoTiO_4.

Material	Crystal system	Average Crystallite size (nm)	a (Å)	b (Å)	c (Å)
Ag_2CoTiO_4	Hexagonal	18.7	3.14	3.16	18.47

size of crystallites was obtained by Scherrer equation (Eq.1) utilizing (012) diffraction peak. In addition, the unit cell parameters were calculated which are provided in Table 1.

$$D = \frac{k\,\lambda}{\beta\,cos\theta} \quad (1)$$

The SEM images at different magnification were provided in Fig. 2a, b. The SEM image at 500 nm resolution displays spherical nanoparticles with partly agglomerated particles (Fig. 2a). Besides, SEM image in higher magnification (Fig. 2b) depicts that the spherical nanoparticles have an average size below 50 nm. The uniformity and nano-sized

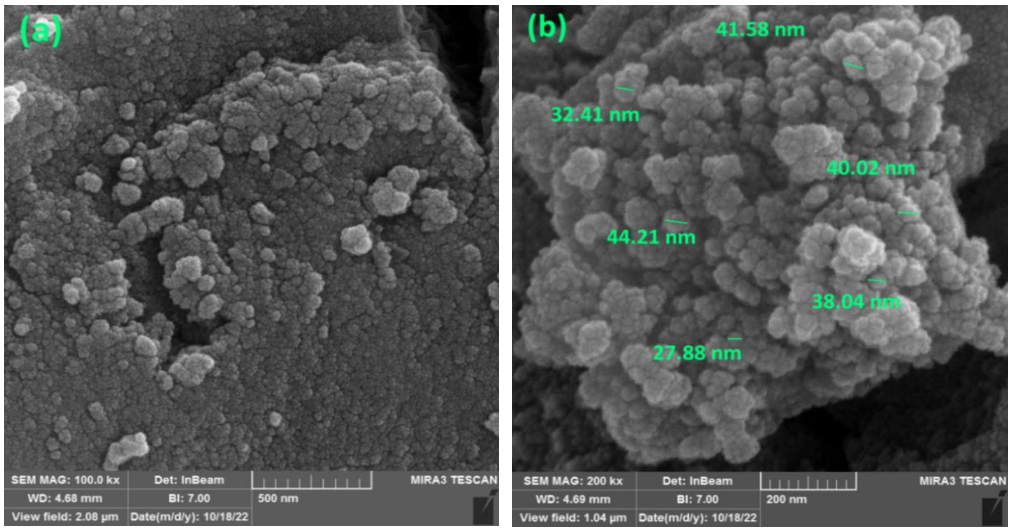

Fig. 2. SEM images for the prepared Ag_2CoTiO_4 nanoparticles at different magnification 500 nm (a) and 200 nm (b).

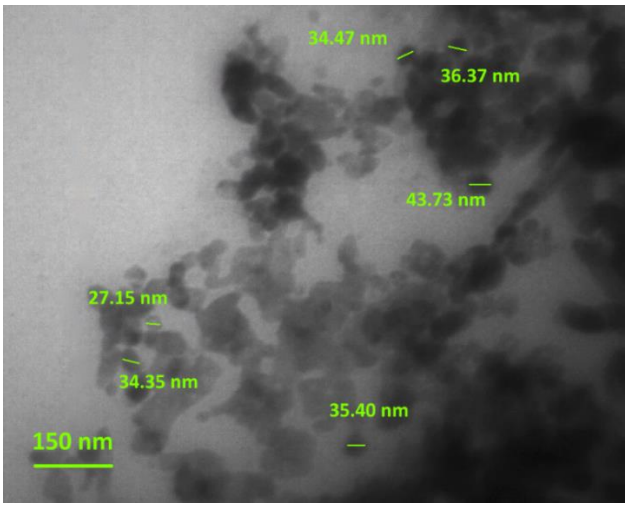

Fig. 3. TEM image for the prepared Ag_2CoTiO_4 nanoparticles.

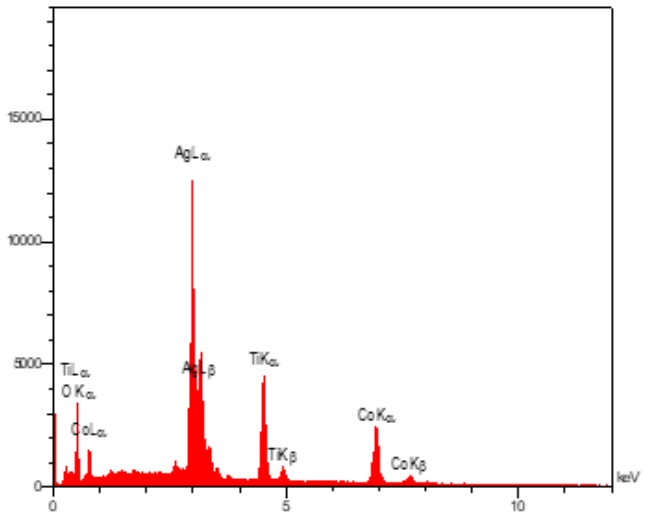

Fig. 4. EDX spectrum for the prepared Ag_2CoTiO_4.

particles are attributed to the utilizing of PEG as an effective capping agent in the preparation method.

Also, the morphological feature of Ag_2CoTiO_4 nanoparticles was further studied by TEM image, as shown in Fig. 3. The spherical nanoparticles are clearly observed in TEM image with the average size below 50 nm.

In order to investigate the composition and elemental analysis, the prepared ACTO nanoparticles were studied by the EDX spectroscopy. Fig. 4 represents the EDX spectrum which clearly testify the presence of the Ag (54.27 wt%), Co (14.87 wt%), Ti (13.21 wt%) and O (17.65 wt%) elements.

The chemical groups were investigated for the prepared ACTO nanoparticles using FT-IR spectroscopy, as shown in Fig. 5. The formation of metal-oxygen (M-O) bonds is confirmed by absorption peaks at 687 cm^{-1}, 623 cm^{-1} and 559 cm^{-1} [10]. Also, O-H vibration peaks are observed at a broad peak centered 3300 cm^{-1} and a weak absorption peak at 1603 cm^{-1} [11]. Due to exposure

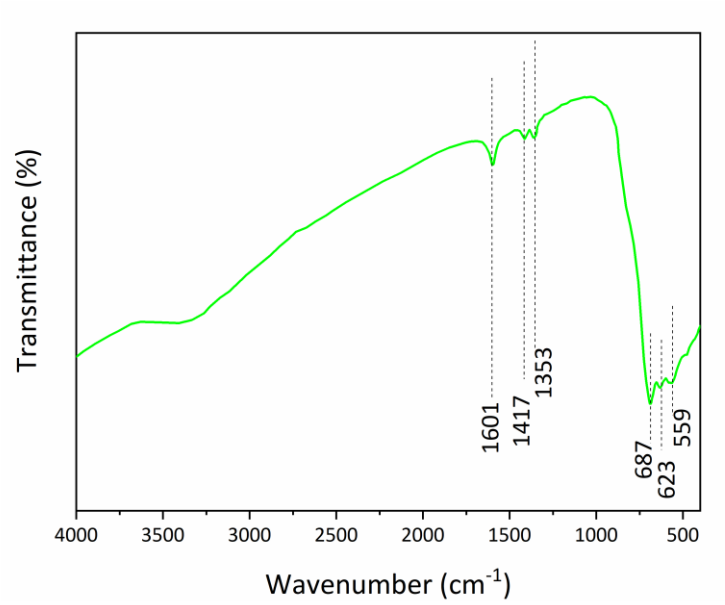

Fig. 5. FT-IR spectrum for the prepared Ag_2CoTiO_4.

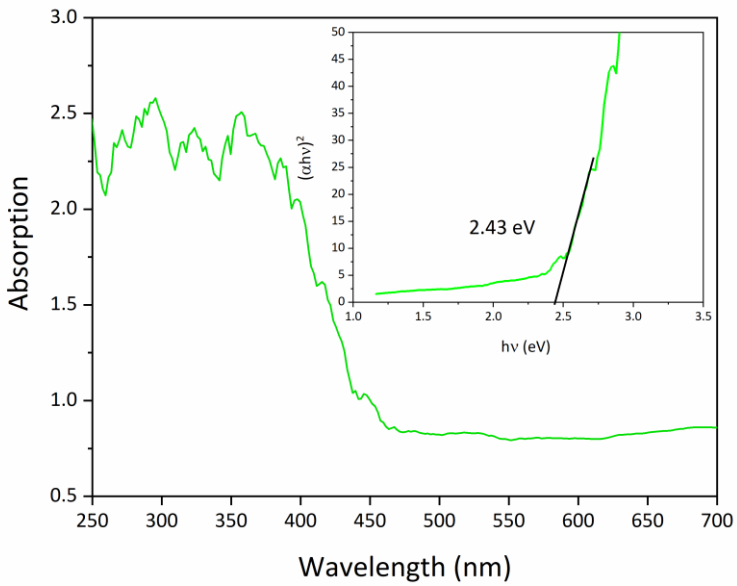

Fig. 6. DRS spectrum for the prepared Ag_2CoTiO_4 nanoparticles. The inset shows $(\alpha h\nu)^2$ vs. hν plot of the prepared nanoparticles.

of bare surface of the prepared nanoparticles to atmosphere, the absorbed carbon species are traced at the two absorption peaks at 1417 cm^{-1} and 1353 cm^{-1} which are assigned to the asymmetric stretching vibration of the carbonate groups [12].

The optical properties of the prepared ACTO nanoparticles were studied using DRS analysis which shown in Fig. 6. As seen in DRS spectrum, the ACTO possess a remarkable absorption in visible light region (400-700 nm). The intensified absorption peak in the range of 200-300 nm relates to the ligand to metal charge transfer transitions [13]. Moreover, the band-gap energy of the prepared ACTO nanoparticles was obtained by plotting $(\alpha h\nu)^2$ vs. hν, which provided in inset to Fig. 6. Clearly, the ACTO nanoparticles have the appropriate band-gap energy (2.43 eV) which affirms the prosperity of the ACTO for conducting the photocatalytic reaction under visible light irradiation.

Photocatalytic experiments

The Photocatalytic studies were performed over the prepared ACTO nanoparticles under different experimental conditions. An aqueous solution of acid red 88 (AR 88) with constant concentration of 50 ppm was used in all the photocatalytic reactions as a model of wastewater contaminated with organic pollutant. Illumination of the photocatalytic system was carried out using two LED lamps (100 W). The distance of reaction vessel from light source was kept constant as 20 cm. Before the illumination, the photocatalyst material was dispersed into the dye solution and then kept in darkness for 15 min to reach adsorption/desorption equilibrium.

The concentration of AR 88 was monitored at a constant time interval of 30 min using UV-Vis spectrophotometer at maximum wavelength of 506 nm. The photocatalyst particles were separated from the dye solution using centrifugation at 6000 rpm for 10 min.

The photocatalytic reactions were conducted under different loaded amounts of photocatalyst material (0, 0.03, 0.06 and 0.09) and concentration of H_2O_2 (0 mL, 2 mL, 4 mL, 6 mL and 8 mL).

The results of photocatalytic experiments are shown in Fig. 7. The UV-Vis absorption of the AR 88 solution under different reaction time over 30 mg of the loaded photocatalyst was provided in Fig.7a. As clearly seen, the intensity of absorption peaks decreases as the reaction vessel is exposed to higher illumination time.

Fig. 7b shows the photocatalytic degradation results under different amounts of photocatalyst material. As expected, the degradation efficiency decreases with increasing the amount of ACTO photocatalyst. This observation could be attributed to the reduced penetration of light beam into more

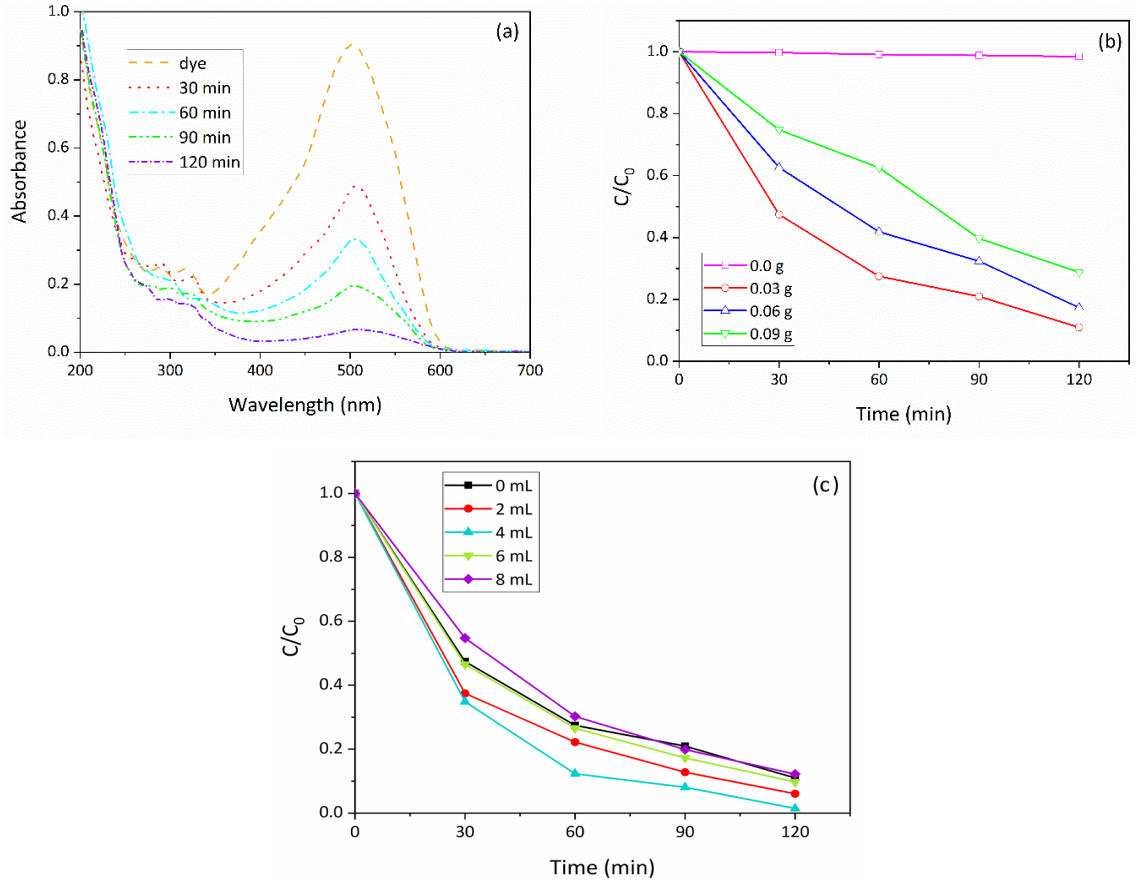

Fig. 7. Photocatalytic reaction results for degradation of AR 88: UV-Vis absorption of AR 88 over the ACTO photocatalyst at different irradiation time (a), effect of different amount of loaded photocatalyst (b) and effect of different added amount of H_2O_2 (c).

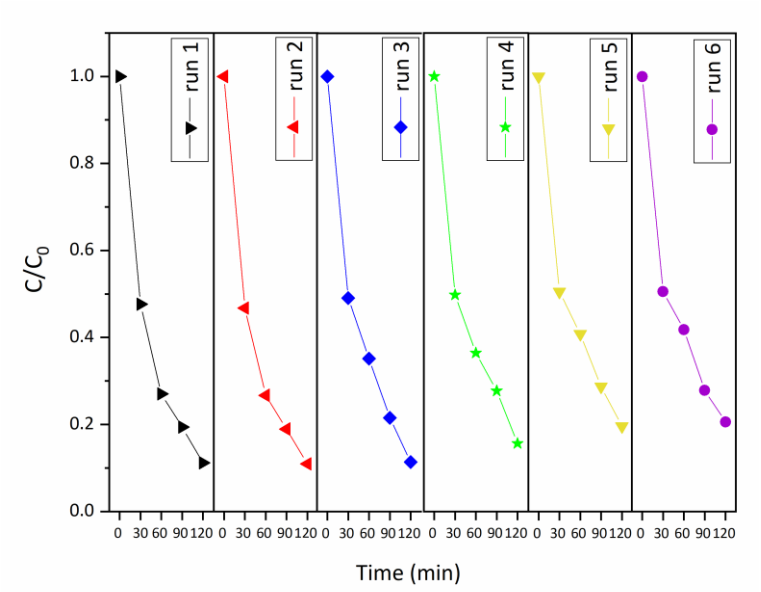

Fig. 8. Recyclability experiment for degradation of AR 88 over the prepared ACTO photocatalyst.

turbid dye solution [14]. The highest photoactivity (89.02%) was obtained using 30 mg the prepared ACTO photocatalyst.

Fig. 7c depicts the effect of different amount of H_2O_2 on the photocatalytic degradation of AR 88 solution (50 ppm) over ACTO photocatalyst (30 mg). Although the photocatalytic activity increases using addition of H_2O_2, the higher concentration of H_2O_2 leads to a decline in the photocatalytic degradation of AR 88 solution. At moderate concentration, H_2O_2 could well cooperate to produce hydroxyl radical (Eq.2) which causes to more degradation of AR 88. However, further amount of hydrogen peroxide can act as a radical scavenger which reacts with hydroxyl radicals to form inactive or less active species (Eq. 3, 4) [15, 16].

$$TiO_2\,(e^-) + H_2O_2 \longrightarrow TiO_2 + OH^- + OH^\circ \quad (2)$$

$$H_2O_2 + OH^\circ \longrightarrow HO_2^\circ + H_2O \quad (3)$$

$$HO_2^\circ + OH^\circ \longrightarrow H_2O + O_2 \quad (4)$$

Moreover, the recyclability experiments were conducted to study the stability and efficiency of the prepared photocatalyst in consecutive reactions. After each reaction cycle, the photocatalyst particles were collected using centrifugation at 6000 rpm and the washed several time by ethanol/distilled water solution. The recovered photocatalyst particles were dried in an oven at 70 °C for 2 hours.

Fig. 8 shows the photocatalytic efficiency of the ACTO photocatalyst in 6 successive reaction cycles. As shown, the photocatalyst has a great stability, but there is still some decline in the photoactivity (9.63%) after the 6 successive reaction cycles.

CONCLUSION

This work reports the sol-gel preparation of Ag_2CoTiO_4 delafossite nanoparticles. The great optical and photocatalytic properties of the nanoparticles make them appropriate for employing in the photocatalytic degradation process. The aqueous solution of AR 88 was treated using by the prepared nanoparticle under visible light irradiation. After performing accurate photocatalytic reactions, it reveals that the prepared nanoparticles have a great potential for degradation of AR 88. The photocatalytic degradation of the AR 88 was reached to 89.02% after 120 min visible-light illumination. The recyclability experiment shows the prepared photocatalyst has a great stability in 6 reaction cycles.

ACKNOWLEDGEMENTS

The authors would like to acknowledge the financial support of this work by the Azad University, Tehran, Iran.

CONFLICT OF INTEREST

The authors declare that there is no conflict of interests regarding the publication of this manuscript.

REFERENCES

1. Li Y, Zhang Y, Qian K, Huang W. Metal–Support Interactions in Metal/Oxide Catalysts and Oxide–Metal Interactions in Oxide/Metal Inverse Catalysts. ACS Catalysis. 2022;12(2):1268-1287.
2. Yu M, Draskovic TI, Wu Y. Cu(i)-based delafossite compounds as photocathodes in p-type dye-sensitized solar cells. Physical Chemistry Chemical Physics. 2014;16(11):5026.
3. Sheets WC, Stampler ES, Bertoni MI, Sasaki M, Marks TJ, Mason TO, et al. Silver Delafossite Oxides. Inorganic Chemistry. 2008;47(7):2696-2705.
4. Chen Z-J, Guo H, Liu H-Y, Niu C-G, Huang D-W, Yang Y-Y, et al. Construction of dual S-scheme $Ag_2CO_3/Bi_4O_5I_2/g\text{-}C_3N_4$ heterostructure photocatalyst with enhanced visible-light photocatalytic degradation for tetracycline. Chem Eng J. 2022;438:135471.
5. Jiang X, Chen S, Zhang X, Qu L, Qi H, Wang B, et al. Carbon-doped flower-like Bi_2WO_6 decorated carbon nanosphere nanocomposites with enhanced visible light photocatalytic degradation of tetracycline. Research Square Platform LLC; 2022.
6. Lee S-Y, Park S-J. TiO_2 photocatalyst for water treatment applications. Journal of Industrial and Engineering Chemistry. 2013;19(6):1761-1769.
7. Dong H, Zeng G, Tang L, Fan C, Zhang C, He X, et al. An overview on limitations of TiO_2-based particles for photocatalytic degradation of organic pollutants and the corresponding countermeasures. Water Res. 2015;79:128-146.
8. Karati A, Parida T, Gupta J, Adigilli HK, Borse PH, Joardar J. Band-gap engineering in novel delafossite-type multicomponent oxides for photocatalytic degradation of methylene blue. Materials Research Bulletin. 2021;137:111181.
9. Guo J, Jiang L, Liang J, Xu W, Yu H, Zhang J, et al. Photocatalytic degradation of tetracycline antibiotics using delafossite silver ferrite-based Z-scheme photocatalyst: Pathways and mechanism insight. Chemosphere. 2021;270:128651.
10. Viana MM, Soares VF, Mohallem NDS. Synthesis and characterization of TiO_2 nanoparticles. Ceram Int. 2010;36(7):2047-2053.

11. Kumar PM, Badrinarayanan S, Sastry M. Nanocrystalline TiO_2 studied by optical, FTIR and X-ray photoelectron spectroscopy: correlation to presence of surface states. Thin Solid Films. 2000;358(1-2):122-130.
12. Thirumalairajan S, Girija K, Ganesh I, Mangalaraj D, Viswanathan C, Balamurugan A, et al. Controlled synthesis of perovskite $LaFeO_3$ microsphere composed of nanoparticles via self-assembly process and their associated photocatalytic activity. Chem Eng J. 2012;209:420-428.
13. Colón G, Maicu M, Hidalgo MC, Navío JA. Cu-doped TiO_2 systems with improved photocatalytic activity. Applied Catalysis B: Environmental. 2006;67(1-2):41-51.
14. Sathish Kumar PS, Sivakumar R, Anandan S, Madhavan J, Maruthamuthu P, Ashokkumar M. Photocatalytic degradation of Acid Red 88 using Au–TiO_2 nanoparticles in aqueous solutions. Water Res. 2008;42(19):4878-4884.
15. Daneshvar N, Salari D, Khataee AR. Photocatalytic degradation of azo dye acid red 14 in water on ZnO as an alternative catalyst to TiO_2. J Photochem Photobiol A: Chem. 2004;162(2-3):317-322.
16. Cater SR, Stefan MI, Bolton JR, Safarzadeh-Amiri A. UV/H_2O_2 Treatment of Methyl-tert-Butyl Ether in Contaminated Waters. Environmental Science & Technology. 2000;34(4):659-662.